



## Research Article

# Adsorptive removal of biochemical oxygen demand (BOD<sub>5</sub>) and chemical oxygen demand (COD) from greywater using activated carbon prepared from tropical almond and palm kernel shells

Michael Oteng-Peprah<sup>1\*</sup>, Benjamin Agyei-Tuffour<sup>2</sup>, Maame Adwoa Animpong<sup>3</sup>, Frank Nana Osei<sup>4</sup>, Deborah Oyiye-Mensah<sup>5</sup>, Mike Agbesi Acheampong<sup>6</sup>

<sup>1</sup>Department of Water and Sanitation, School of Physical Sciences, University of Cape Coast, Cape Coast, Ghana

<sup>2</sup>Department of Materials Engineering, University of Ghana, Legon, Ghana

<sup>3</sup>Centre for Scientific and Industrial Research, Industrial Research Institute, Accra, Ghana

<sup>4</sup>Faculty of Built and Natural Environment, Takoradi Technical University, Takoradi Ghana

<sup>5</sup>Waste Alliance, Accra, Ghana

<sup>6</sup>Department of Chemical Engineering, Kumasi Technical University, Kumasi, Ghana

E-mail: moteng-peprah@ucc.edu.gh

**Received:** 17 November 2023; **Revised:** 12 December 2023; **Accepted:** 13 December 2023

**Abstract:** This study assesses the reduction of 5-day biochemical oxygen demand (BOD<sub>5</sub>) and chemical oxygen demand (COD) of household greywater using palm kernel activated carbon (PKAC) and tropical almond activated carbon (TAAC) produced from locally available materials in a kiln at 800°C and activated using steam at a flowrate of 120 mL hr<sup>-1</sup>. Brunauer-Emmet-Teller (BET) surface area determination revealed that PKAC had a larger surface area than TAAC. Scanning electron microscope (SEM) imagery of the carbons also revealed amorphous and large internal shapes for TAAC while crystalline and closed packed shapes for PKAC. X-ray diffraction (XRD) analysis indicated that the major component present in the PKAC and TAAC was carbon and other allotropes of carbon. Batch results showed that reduction of BOD<sub>5</sub> and COD was affected by particle size. The maximum percentage reduction of BOD<sub>5</sub> and COD by PKAC was 76% and 65% respectively while reduction by TAAC was 62% and 52% respectively. The adsorption process was well described by the Freundlich adsorption isotherm. The studies showed that PKAC is a better adsorbent for reducing BOD<sub>5</sub> and COD from domestic greywater as compared with TAAC. The PKAC is a potential low-cost adsorbent for BOD<sub>5</sub> and COD removal from domestic greywater.

**Keywords:** palm kernel; tropical almond; activated carbon; biochemical oxygen demand; chemical oxygen demand, adsorption

## 1. Introduction

Rapid urbanization in most developing countries has led to a rise in water demand in most towns and villages. Associated with this rise in demand is an increase in volumes of wastewater generated. Most developing countries lack the technical and non-technical competences to manage the wastewater generated and this leads to indiscriminate discharge of wastewater into the environment. Many studies (1-6) have revealed wastewater generation rates between 20-80 L p<sup>-1</sup> d<sup>-1</sup> in some developing countries. Greywater which accounts for a large

Copyright ©2023 Michael Oteng-Peprah, et al.

DOI: <https://doi.org/10.37256/2120233945>

This is an open-access article distributed under a CC BY license  
(Creative Commons Attribution 4.0 International License)

<https://creativecommons.org/licenses/by/4.0/>

percentage of the domestic wastewater generated and is often contaminated with different hazardous materials both as organic and inorganic compounds (3, 7, 8). These organic and inorganic wastes originate from many sources such as human waste, food waste, washing and personal hygiene product (9, 10). A recent study has revealed that greywater composition is affected by the hygienic practices, cooking methods, type of use and quality of the raw water (6). During decomposition of organic matter in greywater, the oxygen concentration is depleted due to the high organic loads found in greywater. This leads to low oxygen concentration in receiving water bodies and eventually deprives other aquatic organisms of oxygen needed for survival. In order to reduce the impact of organic loads caused by high BOD<sub>5</sub> and COD, it is imperative for greywater to be treated before being finally discharged into natural waters. Conventional processes of treating greywater before reuse or final disposal are limited or non-existent in many developing countries. These conventional systems are expensive to install and mostly require an extensive network of piping coupled with its associated management protocols. The non-availability of these treatment systems exposes the environment to contaminants associated with unregulated greywater discharge and its effect on plants and animals. Advocacy for household greywater treatment before discharge has been very limited or non-existent in many developing countries and as such greywater is mostly discharge untreated into the environment. This may be due to both technical and non-technical challenges associated with managing treatment systems at the household level. In order to encourage greywater treatment at the household level, there is the need to provide an alternative low-cost solution for greywater treatment and reuse.

Adsorption process which is a physico-chemical process has remained one of the most widely used techniques for treating water and wastewater and has proven to be very useful in many studies (11-14). It has remained one of the most efficient and important methods on condition that the adsorbent used is cheap and locally available and does not require further pre-treatment steps. In order to promote household greywater treatment and reuse, there is the need to provide an alternative low cost and sustainable solution. Activated carbon has proven to be an effective adsorbent in wastewater treatment due to its high surface area, high adsorptive capacity and its large microporous structure (15). It can be prepared from a large number of low-cost sources and agricultural wastes such as rice husk, apricot, bamboo, date pal, residue, avocado (16). Tropical almond and palm kernel shell are a considerable part of the abundant agricultural waste materials within found in many developing countries. Many researchers have investigated the performance of palm kernel activated carbon on removal of certain wastewater parameters (17-21) but studies of its effect on removal of BOD<sub>5</sub> and COD have remained scanty or non-existent. Tropical almond, a fruit with a mesocarp, has not been explored in its application for use as activated carbon. This agricultural product, which is very common in most tropical countries, is discarded as waste or burnt in the open. Though there are other equally efficient processes such as filtration, sedimentation, coagulation that can be used to treat greywater, the choice of adsorption is based on the availability these agricultural waste materials which can be put to beneficial use. Moreover, the adsorption process is selective and it can also remove a wide range of pollutants including organic and inorganic materials (22). Adsorption systems often have more compact design requiring less space as compared with large scale filtration and coagulation systems. The carbon can be regenerated after exhaustion which is not the case for filtration and coagulation systems (23, 24). In recent times, there has been awareness on the environmental impact created by organic loads which is represented by high BOD<sub>5</sub> and COD on freshwater resources. This study explores the potential of tropical almond activated carbon (TAAC) and palm kernel activated carbon (PKAC) in the removal of BOD<sub>5</sub> and COD from domestic greywater.

## 2. Methods

### 2.1 Material processing

The palm kernel shell was obtained from a local palm oil mill and the tropical almond fruits were obtained from the campus of University of Cape Coast all in Cape Coast Ghana. The almond fruits were crushed to remove the fleshy mesocarp from the hard endocarp. The hard endocarp is further crushed to reveal the edible kernel. The hard endocarp is the material of interest in this study. These two materials (almond shell and palm kernel shell) were cleaned several times with distilled water to eliminate any dirt and water-soluble impurities. The cleaned shells were then airdried in a laboratory drier for 8hours and then further oven dried at 110°C in a Heratherm gravity convection laboratory oven for 24hours in order to remove any surface moisture. The dried samples were then size reduced to desired sizes (2-6mm) using a laboratory crusher (Morse 8x8 Jaw Crusher) and sieves (sigma Aldrich). The activated carbons were prepared by physical activation with steam at 800°C and steam flowrate at 120 mL hr<sup>-1</sup>. After the activation process, the samples were taken out and washed with distilled water to remove any residual ash that might be on the carbons. Greywater was collected from different households within the central region of Ghana and a composite is formed for the sorption experiment.

## 2.2 Material processing

The pH, was measured on site using a Horiba U-50 multi parameter water quality meter. The five-day biochemical oxygen demand (BOD<sub>5</sub>) concentration was determined using the Lovibond BD 606 BOD system. The concentration of chemical oxygen demand (COD) was determined using the closed reflux colorimetric method as stated in (25) 5220C. The initial pH of the greywater was 7.4.

### 2.2.1 Sorption experiment

All experiments were carried out at ambient temperature (25°C) in batch mode. The batch experiments were conducted in Erlenmeyer flasks of 1000ml capacity using an orbital shaker at a speed of 400 rev min<sup>-1</sup> as recommended by Nayl, Elkhashab (16).

### 2.2.2 Greywater pre-treatment

The greywater collected were first filtered through a laboratory sand filter to reduce the total suspended solids (TSS) content. The BOD<sub>5</sub> and COD of the greywater is determined for the basis of establishing the initial BOD<sub>5</sub> and COD concentrations of the sample. The initial BOD<sub>5</sub> and COD concentration of the greywater samples were 252 mg L<sup>-1</sup> and 421 mg L<sup>-1</sup> respectively.

### 2.2.3 Effect of particle size

The optimum dosage of the two materials were weighed and added to two sets of 3 different 1000ml Erlenmeyer flasks. The first, second and third contain 2mm, 4mm and 6mm average particle sizes respectively of the material. These flasks were agitated at 400 rev min<sup>-1</sup> for 180mins at room temperature and a pH of 7.4. 500ml from each flask is sampled and filtered and the filtrate analyzed for BOD<sub>5</sub> and COD.

### 2.2.4 Dosage determination

Batch sorption experiments were carried out using specified weights of both materials 1 g L<sup>-1</sup> to 10 g L<sup>-1</sup> with increases of 1g for each experiment and mixed with 1000ml of greywater in 1000ml Erlenmeyer flasks. The setup consisted of 10 Erlenmeyer flasks for each of the materials. The mixtures were agitated continuously using an orbital shaker at the following conditions: 400 rev min<sup>-1</sup>, temperature of 25°C, pH = 7.4, time of agitation = 180mins, particle size = 2mm. 500ml of the solution was collected after the sorption period of 180mins and filtered with a Whatman filter paper and the BOD<sub>5</sub> and COD concentrations measured. The optimum dosage is the sample with the lowest BOD<sub>5</sub> and COD values recorded.

### 2.2.5 Effect of contact time

The optimum dosage (8g L<sup>-1</sup>) and optimum particle size (2mm) of the two materials are weighed and added to two sets of 7 different 1000ml Erlenmeyer flasks containing 1000ml of the greywater each. The first, second, third, fourth, fifth, sixth and seventh flasks was agitated for 10, 30, 60, 90, 120, 150, 180mins respectively. 500ml of each flask is filtered for analysis of BOD<sub>5</sub> and COD.

## 2.3 Characterization of the materials

The density of the materials was determined by using an ultra-pycnometer 1000 after it had been dried at 105°C in an oven for 24hours. The surface area S<sub>BET</sub> was determined using a Micromeritics tristar 3000 system. The scanning electron microscopy (SEM) and x-ray microanalysis was done using a Hitachi TM – 1000 microscope and quantax energy dispersive x-ray spectrometry system respectively. The XRD was determined by using a Bruker D2 phaser x-ray diffractometer.

## 2.4 Calculations

The percentage of removal, thus uptake per gram and equilibrium concentrations of sorbent were calculated using equations 1, 2 and 3

$$R\% = \frac{C_o - C_t}{C_o} \times 100 \quad (1)$$

$$q_t = (C_o - C_t) \frac{V}{m} \quad (2)$$

$$q_e = (C_o - C_e) \frac{V}{m} \quad (3)$$

where  $q_t$  shows the amount of COD and BOD<sub>5</sub> adsorbed by the sorbents at time  $t$ .  $C_o$ ,  $C_t$  and  $C_e$  represents the COD and BOD<sub>5</sub> concentrations in the solution ( $\text{mg L}^{-1}$ ) at initial time, instantaneous time  $t$ , and equilibrium respectively.  $V$  represents the volume of solution (L) and  $m$  is the mass of the sorbent (g).

## 2.5 Mathematical equations and models of adsorption isotherms

These are expressions or relationship curves that describes the conditions under which sorption equilibrium is reached at a constant temperature. These isotherms can be used to compare the adsorptive properties of different adsorbents under varying conditions. They further provide insight into the mechanisms involved in the sorption process.

### 2.6 Linear isotherm

$$q_e = \frac{x}{m} = k_p C_e \quad (4)$$

where  $x/m$  represents the amount adsorbed by unit mass ( $\text{mg g}^{-1}$ )

### 2.7 The Freundlich isotherm model

It is represented by the following equation:

$$q_e = K_F C_e^{1/n} \quad (5)$$

In its linear form, it assumes the following state:

$$\log q_e = \log K_F + \frac{1}{n} \log C_e \quad (6)$$

where  $q_e$  is equal to the uptake ( $\text{mg g}^{-1}$ ) at equilibrium,  $K_F$  is a measure of the sorption capacity,  $1/n$  is the sorption intensity, and  $C_e$  is the final BOD<sub>5</sub> or COD concentration in solution ( $\text{mg L}^{-1}$ ). The Freundlich isotherm constants  $K_F$  and  $1/n$  are evaluated from the intercept and the slope respectively, of the linear plot  $\log q_e$  against  $\log C_e$

### 2.8 Langmuir isotherm model

It is represented by the following set of equations

$$q_e = \frac{q_m K_L C_e}{1 + K_L C_e} \quad (7)$$

where  $q_e$  is the amount adsorbed per specific amount of adsorbent ( $\text{mg g}^{-1}$ ),  $C_e$  is the equilibrium concentration of the solution ( $\text{mg L}^{-1}$ ) and  $q_m$  is the maximum amount required to form a monolayer ( $\text{mg g}^{-1}$ ). The Langmuir equation can be rearranged to a linear form for the convenience of plotting and determination of the Langmuir constant ( $K_L$ ) as below. The values of  $q_m$  and  $K_L$  can be determined from the linear plot of  $C_e/q_e$  versus  $C_e$ .

$$\frac{C_e}{q_e} = \frac{1}{K_L q_m} + \frac{1}{q_m} C_e \quad (8)$$

The essential characteristics of the Langmuir isotherm parameters can be used to predict the affinity between the sorbate and the sorbent using the separation factor or dimensionless equilibrium parameter  $R_L$  expressed as in the following equation

$$R_L = \frac{1}{1 + K_L C_o} \quad (9)$$

where  $K_L$  is the Langmuir constant and  $C_o$  is the initial concentration. The value of the separation factor  $R_L$  provides important information about the nature of adsorption. The value of  $R_L$  is between 0 and 1 for favourable adsorption, while  $R_L > 1$  represents unfavourable adsorption and  $R_L = 1$  represents linear adsorption.

### 2.9 Dubinin-Radishkevich isotherm (D-R) model

This is represented in the linear form by the equation

$$\ln q_e = \ln Q_D - B_D(RT \ln(1 + \frac{1}{C_e}))^2 \quad (10)$$

where  $Q_D$  is the theoretical maximum capacity ( $\text{mol g}^{-1}$ ),  $B_D$  is the D-R model constant ( $\text{kJ mol}^{-1} \text{K}^{-1}$ ),  $T$  is the absolute temperature (K) and  $R$  is the gas constant ( $\text{kJ mol}^{-1}$ ). The value of  $Q_D$  and  $B_D$  can be obtained from the intercept and slope of the plot of  $\ln(q_e)$  versus  $\ln(1+1/C_e)$ . The mean energy of sorption,  $E$  ( $\text{kJ mol}^{-1}$ ) is calculated from the relation

$$E = \frac{1}{\sqrt{2B_D}} \quad (11)$$

## 2.10 Temkin

This is represented in the linear form as:

$$q_e = \frac{RT}{b_T} \ln K_T + \frac{RT}{b_T} \ln C_e \quad (12)$$

where  $K_T$  ( $\text{L g}^{-1}$ ) is the Temkin isotherm constant,  $b_T$  ( $\text{J mol}^{-1}$ ) is a constant related to the heat of sorption and  $R$  ( $8.314 \text{ J/mol/K}$ ) is the gas constant. A plot of  $q_e$  versus  $\ln(C_e)$  gives a straight line from which  $K_T$  and  $b_T$  can be evaluated from the slope and intercept.

## 3. Sorption kinetic models

These are mainly used for determination of substances or physical and chemical reactions in the process of adsorption rate control steps. Knowledge about the kinetics of the sorption process facilitates the understanding of the mechanisms involved in the sorption process. The classical models commonly used to study the mechanism of reactions are the pseudo-first-order and pseudo-second-order models.

### 3.1 Pseudo-first order kinetic model

It is represented by the following equations

$$\frac{dq_t}{dt} = k_1(q_e - q_t) \quad (13)$$

Integrating of the above equation with boundary conditions of  $t=0, q_t=0$  and  $t=t, q_t=q_t$  gives the following equation

$$\log(q_e - q_t) = \log q_e - \left(\frac{k_1}{2.303}\right)t \quad (14)$$

where  $q_e$  and  $q_t$  are the amounts of COD or BOD<sub>5</sub> adsorbed at equilibrium and at time  $t$  ( $\text{mg g}^{-1}$ ), respectively,  $t$  is the contact time (min) and  $k_1$  is the pseudo-first-order rate constant (/min). The straight-line plot of  $\log(q_e - q_t)$  against  $t$  gives  $\log(q_e)$  as slope and intercept equal to  $k_1/2.303$ . Hence the amount of solute sorbed per gram of sorbent at equilibrium ( $q_e$ ) and the first order rate constant ( $k_1$ ) can be evaluated from the slope and intercept.

### 3.2 Pseudo-second-order kinetic model

This is represented by the following equations

$$\frac{dq_t}{dt} = k_2(q_e - q_t)^2 \quad (15)$$

Integrating of the above equation with boundary conditions of  $t=0, q_t=0$  and  $t=t, q_t=q_t$  gives the following equation

$$\left(\frac{t}{q_t}\right) = \frac{1}{k_2 q_e^2} + \frac{1}{q_e} t \quad (16)$$

where  $k_2$  represents the rate constant,  $q_t$  is the uptake capacity at any time  $t$

## 4. Results and Discussion

### 4.1 Physical characteristics of the materials

The physical characteristics of the activated carbons are presented in Table 1. The density of palm kernel activated carbon (PKAC) is higher than tropical almond activated carbon (TAAC). The recommended range of densities for activated carbon is within  $0.4\text{-}0.5 \text{ g cm}^{-3}$  (26) which implies that PKAC falls within the recommended

densities for commercial activated carbon. The TAAC, however, could not meet the density requirement for it to be classified as commercial activated carbon. The low density recorded for TAAC could be attributed to its very high fibrous nature, which is an indication that it cannot be used for commercial purposes. The BET surface area obtained showed that the PKAC had a higher surface area  $620 \text{ m}^2 \text{ g}^{-1}$  as compared to TAAC of  $407 \text{ m}^2 \text{ g}^{-1}$ . The surface area of TAAC does not fall within the recommended range of surface area of commercial activated carbon ( $500\text{-}1500 \text{ m}^2 \text{ g}^{-1}$ ). A similar study by Hidayu and Muda (17) on characterization of activated carbon using palm kernel shell obtained surface area of  $584 \text{ m}^2 \text{ g}^{-1}$ . The slight variations in the surface area recorded for this study may be due to the activation method that was used in the different studies. A higher BET generally suggests higher adsorption capacity because the carbon has wider surface to allow for adsorption under different conditions.

**Table 1.** Physical characteristics of the materials

	Density $\text{g cm}^{-3}$	BET Surface Area $\text{m}^2 \text{ g}^{-1}$
TAAC	0.35	407
PKAC	0.46	620

#### 4.2 SEM images of the activated sorbents

Figure 1 and Figure 2 show the SEM images of TAAC and PKAC respectively (6,000 times magnification). Using the scale of  $5 \mu\text{m}$ , it is seen that majority of the particles in the PKAC (Figure 2) are less than  $5 \mu\text{m}$ . It can also be said that the particles are crystalline because they have distinct shapes. However, the TAAC (Figure 1) shows no distinct shape or particle size hence it has an amorphous structure. The pores of the TAAC are large and few and the particles have bulky shape when compared to PKAC. Using the scale, it can be seen that most particles fall below the  $5 \mu\text{m}$  compared to the TAAC where most of the particles fall above the  $5 \mu\text{m}$ .

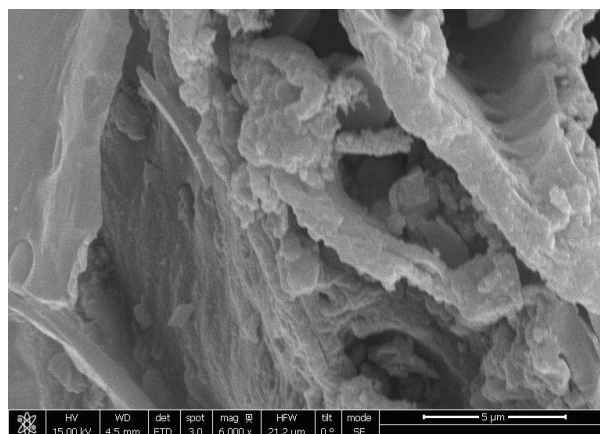


**Figure 1.** SEM image of TAAC

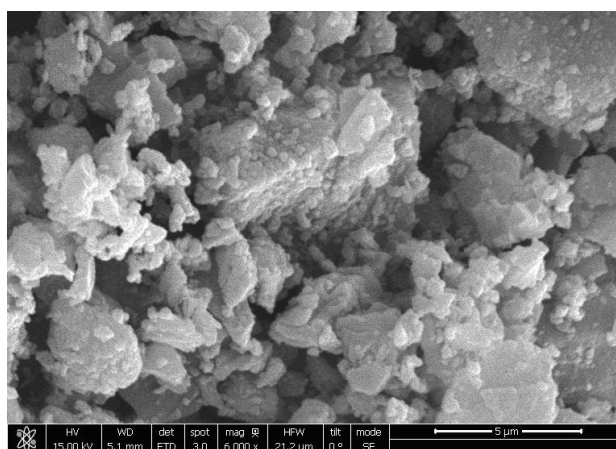


**Figure 2.** SEM image of PKAC

## 4.3 XRD

### 4.3.1 Almond

The powder diffraction spectrum was compared with standard crystallographic data retrieved from the International Centre for Diffraction Data (ICDD) database using the PDF-4+ 2019 program. Because of the amorphous nature of the sample, several phases were observed. The highly probable match for most of the peaks was carbon (C) with reference number 00-026-1077 with  $2\theta$  values of 26.76, 42.94, 44.04, 45.76, 62.82, 66.96 and 77.72° (27) as shown in Figure 3 and Figure 4. Other phases corresponding to C<sub>60</sub> (00-044-0558), C<sub>70</sub> (00-048-1206) and graphite (00-056-0159) were also observed. These are different allotropes of carbon.

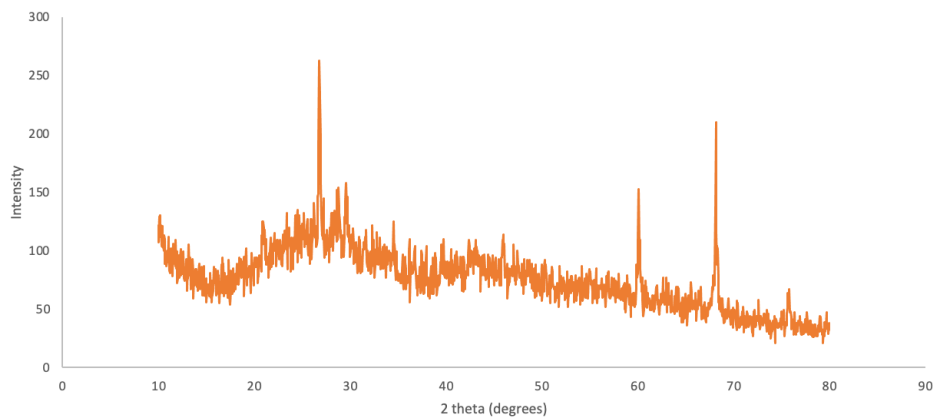


Figure 3. XRD for tropical almond activated carbon

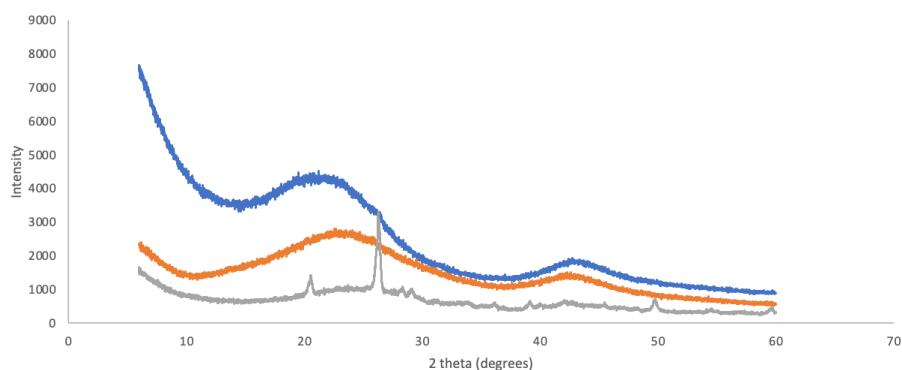


Figure 4. XRD of Palm kernel shell activated carbon

## 4.4 Equilibrium concentrations

The equilibrium concentrations of the study are presented in Table 2. From this table, it can be seen that PKAC had the highest sorption capacity of 34 mg g<sup>-1</sup> in removing COD and 22.88 mg g<sup>-1</sup> in removing BOD<sub>5</sub> as compared with TAAC of 27 mg g<sup>-1</sup> and 19.5 mg g<sup>-1</sup> COD and BOD<sub>5</sub> respectively. These results indicate that PKAC has a higher potential of removing BOD<sub>5</sub> and COD as compared to TAAC. Studies by Nayl, Elkhashab (16) obtained equilibrium concentration of 41.3 mg L<sup>-1</sup> for COD and 20.2 mg L<sup>-1</sup> BOD<sub>5</sub> using activated carbon prepared from date palm.

Table 1. Equilibrium concentrations (qe)

	PKAC	TAAC
BOD (mg/g)	22.88	19.50
COD (mg/g)	34.00	27.00

## 4.5 Effect of particle size

Particle size plays a key role in adsorption studies and this study used three different particle sizes for the sorption experiment. This study was conducted at a pH of 7.4, temperature of 25°C, agitation rate of 400rpm and dosage of 10g L<sup>-1</sup>. Figure 5 shows the percentage removal of BOD<sub>5</sub> and COD for the different particle sizes studied. From the figure, it can be seen that generally the percent removal increased with decreased particle sizes. A similar study also obtained results of increased performance of activated carbon in removing BOD<sub>5</sub> and COD when particle sizes were reduced (28, 29). This may be attributed to an increase in effective specific surface area of the sorbent hence more active sites for adsorption to take place (28). As seen from Figure 5, PKAC shows dominance over TAAC in both BOD<sub>5</sub> and COD removal percentages. This shows that removal of BOD<sub>5</sub> and COD from greywater is considerably affected by changes in particle size as was also reported by Devi, Singh (28).

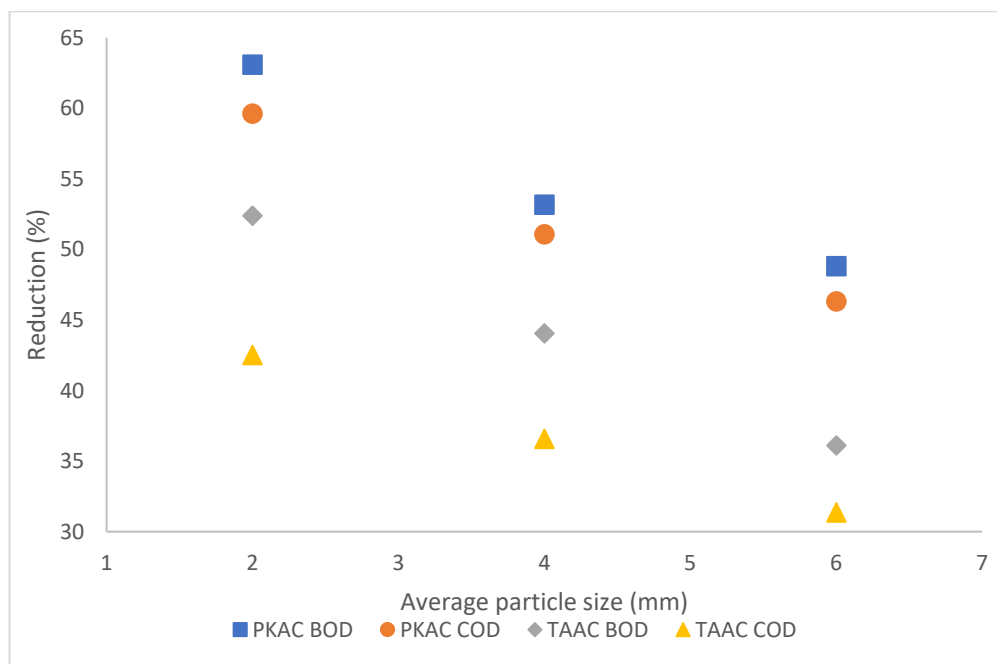


Figure 5. Effect of particle size on BOD<sub>5</sub> and COD reduction

#### 4.6 Effect of adsorbent dose

The effect of carbon dosage on percentage removal of BOD<sub>5</sub> and COD from greywater was conducted at a particle size of 2mm, pH of 7.4, temperature of 25°C, contact time of 210mins and agitation rate of 400rpm. Figure 6 shows the effect of dosage on BOD<sub>5</sub> and COD removal. It can be seen from the figure that generally, the percentage removal of BOD<sub>5</sub> and COD for both TAAC and PKAC increased with increasing dosage of carbon until equilibrium is reached. Equilibrium was reached at about 8 g L<sup>-1</sup> of carbon dose for both PKAC and TAAC. This increase in percent removal with dosage may be due to more active sites available for BOD<sub>5</sub> and COD sorption on the activated carbon which may be attributed to increase in the functional groups and increased surface area as a result of increased dosage (16, 28). With respect to percentage reduction of BOD<sub>5</sub> between the TAAC and PKAC, it can be seen that PKAC is able to remove a higher percentage (72%) of BOD<sub>5</sub> as compared with (65%) for TAAC. COD removal also shows a similar removal pattern observed for BOD<sub>5</sub> removal and this is shown in Figure 6. Comparing the removal rates of the two materials, it can be said that PKAC has a higher capacity of COD removal (66%) as compared to TAAC (58%). This high capacity is supported by the SEM images which show that the PKAC has more porous features than TAAC. This is further supported by the BET results which showed that PKAC has a larger internal surface area as compared to TAAC.



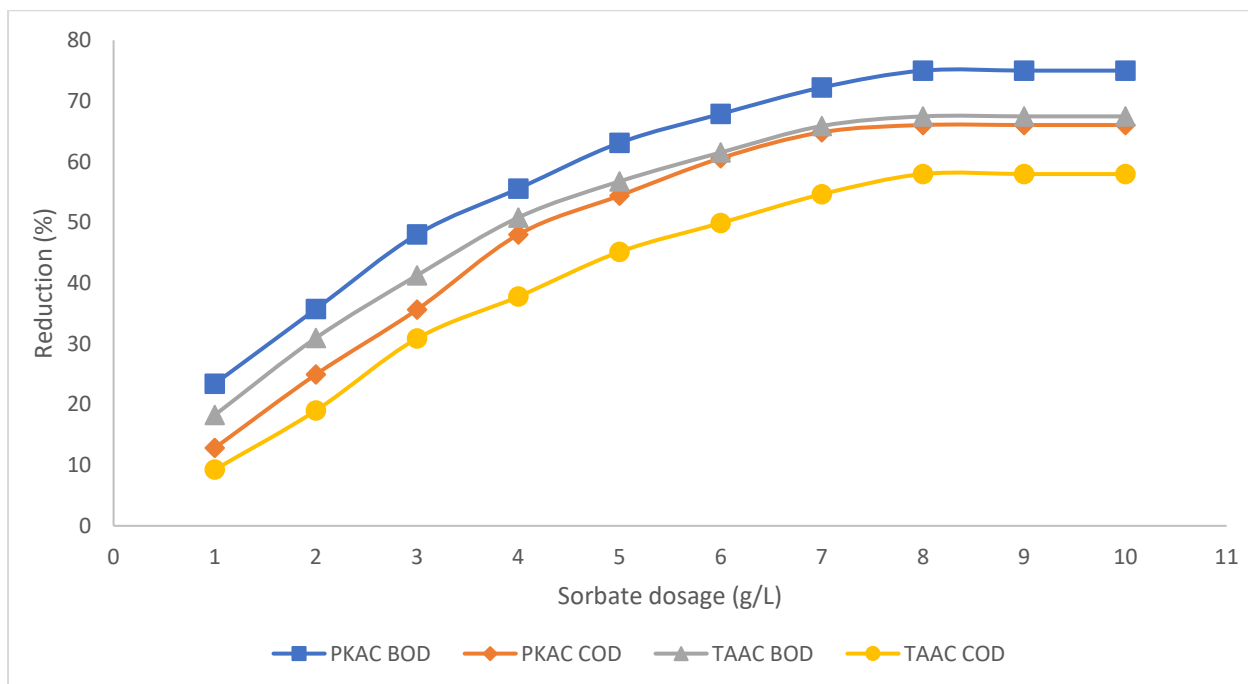


Figure 6. Percentage reduction of BOD<sub>5</sub> and COD against dosage

#### 4.7 Effect of Contact time

The effect of contact time on removal of BOD<sub>5</sub> and COD from greywater was studied at a pH of 7.4, agitation rate of 400rpm, temperature of 25°C and the optimum dosage of 8 g L<sup>-1</sup> and in time periods of 15mins to 210mins (Figure 7). The first 120mins of the reaction showed very rapid reduction of BOD<sub>5</sub> and COD to about 73% and 65% respectively for PKAC and 62% and 52% of BOD<sub>5</sub> and COD respectively for TAAC. Equilibrium was reached at about 150mins for both PKAC and TAAC. The rapid reduction of BOD<sub>5</sub> and COD by the materials may be due to large unoccupied active sites available for adsorption at the initial contact time periods. The smooth nature of the curve may be attributable to the formation of monolayer of BOD<sub>5</sub> and COD over the outer surface of the activated carbon (30). The PKAC removed more BOD<sub>5</sub> and COD than the TAAC under the different time conditions in the study. This might be due to the high surface of the PKAC as shown in the SEM images and also supported by the BET results.

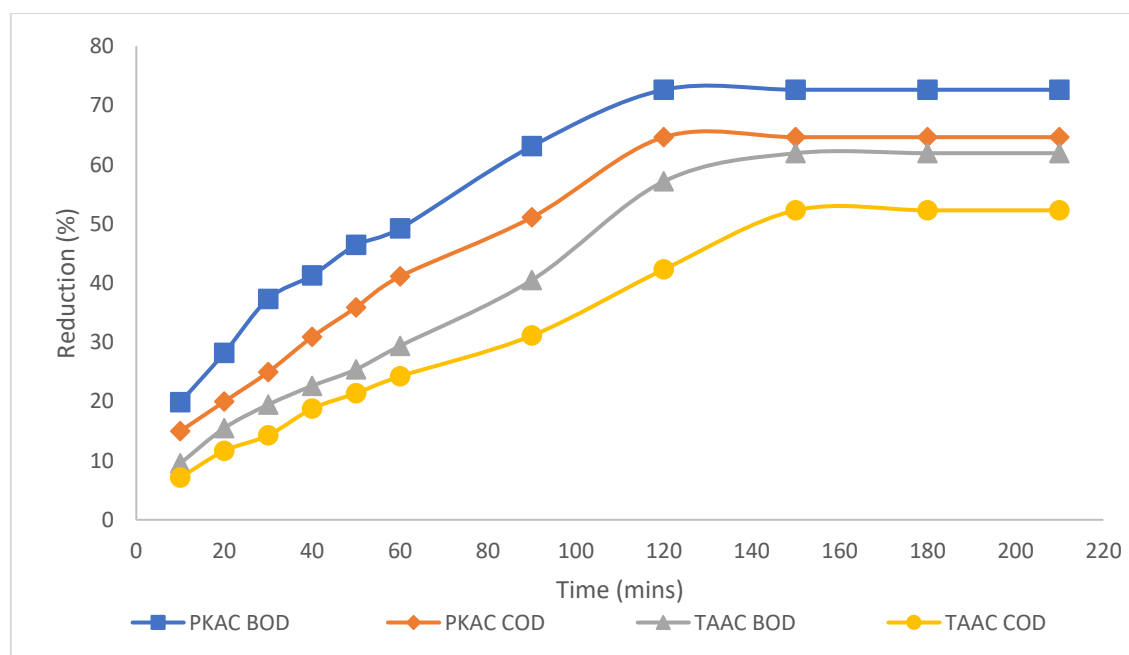


Figure 7. Percentage reduction of BOD<sub>5</sub> and COD against time

#### 4.8 Final concentrations of treated greywater

The initial and final concentrations of the greywater treated under batch conditions using optimum conditions of 8 g L<sup>-1</sup> dosage, 150mins of adsorption time and 2mm particle size is presented in Table 3. It is clear the BOD<sub>5</sub> concentration of the treated greywater for both materials were above the EPA standards for discharge of wastewater into the environment. However, the COD concentrations were all below the EPA standards for discharge of wastewater into the environment. This suggests that within the studied concentrations, there might be the need for further treatment of the greywater to be able to bring the BOD<sub>5</sub> level to the acceptable limits which has been set up by the EPA. Initial and final concentrations of similar studies of BOD and COD after carbon adsorption has been presented in Table 6.

**Table 2.** Initial and final concentrations of greywater after batch treatment

	Initial concentrations		Final concentrations		EPA (31)	
	BOD <sub>5</sub> (mg L <sup>-1</sup> )	COD (mg L <sup>-1</sup> )	BOD <sub>5</sub> (mg L <sup>-1</sup> )	COD (mg L <sup>-1</sup> )	BOD <sub>5</sub> (mg L <sup>-1</sup> )	COD (mg L <sup>-1</sup> )
PKAC	252	421	69	149	50	250
TAAC	252	421	96	201	50	250

#### 4.9 Adsorption isotherms

The experimental data were fitted with the Langmuir, Freundlich, Dubinin-Radushkevich, and Temkin isotherm models and presented in Figures 8, 9, 10 and 11 respectively and the results obtained are presented in Table 4. By using the correlation coefficient, BOD<sub>5</sub> removal using PKAC and TAAC fits well the Freundlich isotherm model (R<sup>2</sup>=0.9820 and 0.9863 respectively) whereas COD removal using PKAC and TAAC fitted the Langmuir isotherm model (R<sup>2</sup>=0.9854 and 0.9054). Similar studies have all reported a good fit of the Freundlich model for BOD<sub>5</sub> removal (16, 28). The fits with Dubinin-Radushkevich and Temkin models were equally good but comparatively less good as compared to the previous fits. The best model describing the fit were the Freundlich and Langmuir models. The adsorption intensity of the Freundlich model 1/n was less than 1 for both materials studied which indicates favourable adsorption (32, 33). This is also supported by the separation factor in the Langmuir model which is between 0 and 1 indicating favourable adsorption. The Q<sub>D</sub> value obtained for the materials indicated that PKAC had a higher sorption capacity for BOD<sub>5</sub> removal as compared to TAAC. The low values of the mean sorption energy show that the forces of attraction are Van der Waal and not chemical bonding which further suggests that the process investigated is a physisorption (34). Results of adsorption isotherms of similar studies have been presented in Table 6.

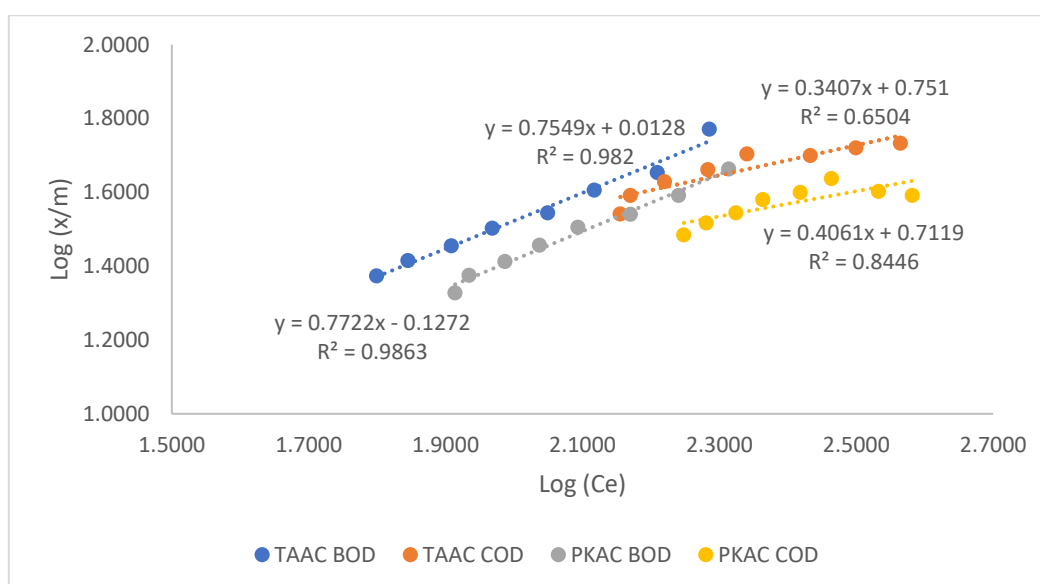


**Figure 8.** Freundlich Isotherm Model

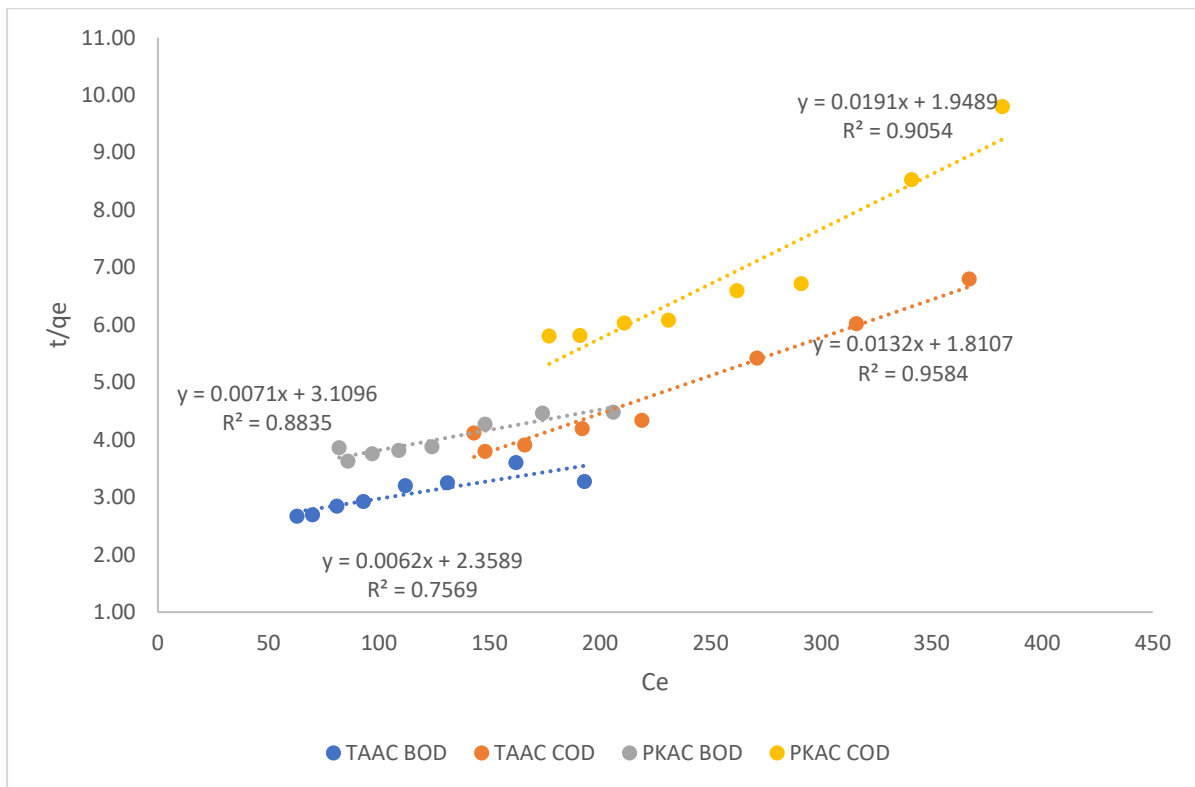


Figure 9. Langmuir Isotherm Model

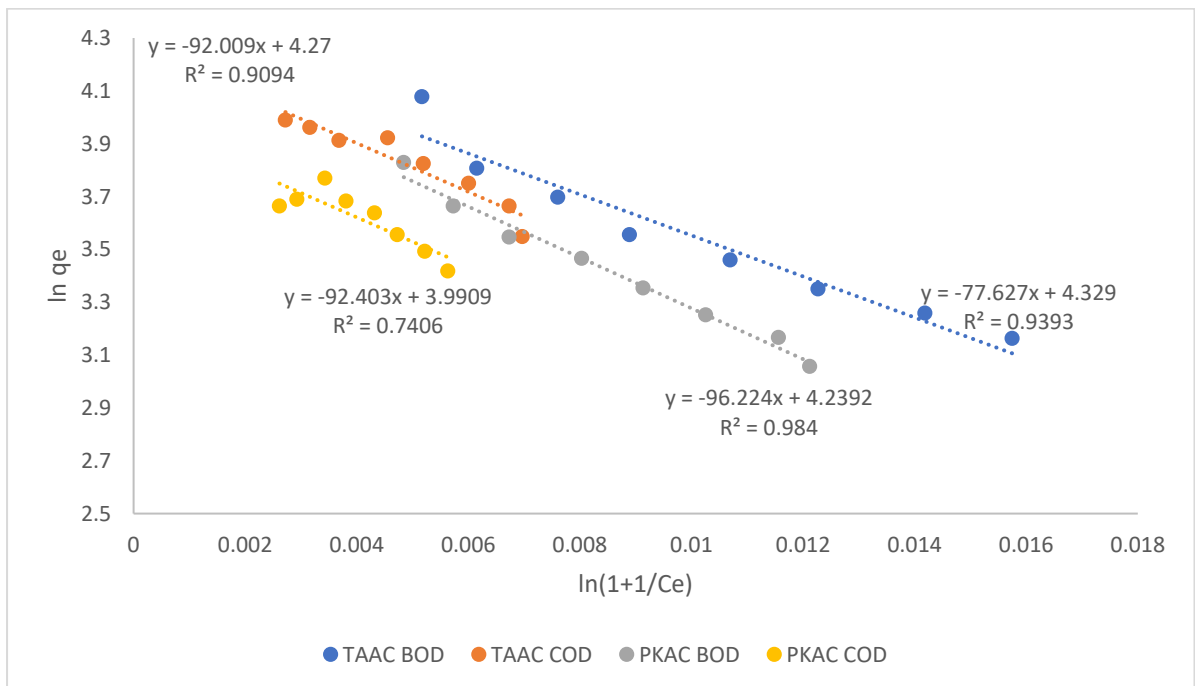


Figure 10. Dubinin-Radushkevich (D-R) Isotherm Model

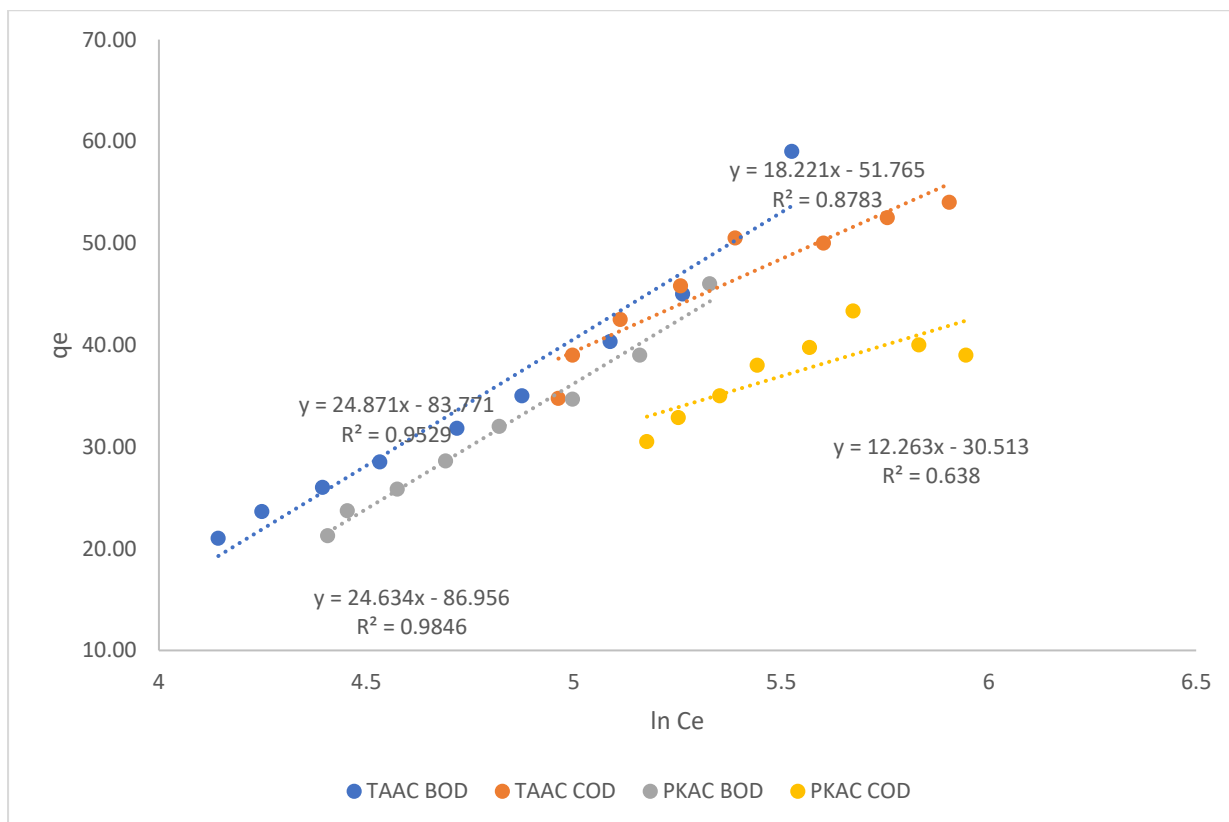


Figure 11. Temkin Isotherm Model

Table 3. Adsorption isotherm parameters

Isotherm parameters	PKAC		TAAC	
	BOD <sub>5</sub>	COD	BOD <sub>5</sub>	COD
<i>Freundlich</i>				
$1/n$	0.7549	0.3407	0.7722	0.4061
$K_F$	1.0299	5.6364	0.7461	5.1511
$R^2$	0.9820	0.6504	0.9863	0.8446
<i>Langmuir</i>				
$q_m$	161.2903	75.7576	140.8541	52.3560
$K_L$	0.0067	0.0039	0.0039	0.0029
$R_L$	0.3710	0.3808	0.5029	0.4504
$R^2$	0.7569	0.9584	0.8835	0.9054
<i>Dubinin-Radushkevich (D-R)</i>				
$Q_D$	4.329	4.27	4.2392	3.9909
$B_D$	0.0157	0.0186	0.0194	0.0186
$E (kJ)$	0.1770	0.1927	0.1971	0.1931
$R^2$	0.9393	0.9094	0.9840	0.7406
<i>Temkin</i>				
$b_T(J)$	99.6169	135.9734	100.5753	202.0364
$K_T$	0.0345	0.0584	0.0293	0.0831
$R^2$	0.9529	0.8783	0.9846	0.6380

#### 4.10 Kinetic adsorption modelling

Different kinetic models have been used to test the experimental data in this study. This is done to understand the mechanism of the adsorption process. Two kinetic models thus Lagrengen pseudo-first-order and pseudo-second-order models were used to fit the experimental data as presented in Figure 6 and figure 7 respectively. This was done in order to determine the model that best fitted the experimental data. The calculated model parameters are presented in Table 5. The BOD<sub>5</sub> and COD removal by PKAC increased rapidly within the first 150minutes of the experiment and then became gradually steady during the last 60minutes of contact time. A maximum removal of 74% and 63% were achieved for BOD<sub>5</sub> and COD respectively. Removal of BOD<sub>5</sub> and COD by TAAC exhibited similar characteristic with rapid removal of BOD<sub>5</sub> and COD within the first 150minutes and gradually steady during the last 60mins of the study. A maximum removal of 56% and 50% was achieved for

BOD<sub>5</sub> and COD respectively. This study therefore shows that the equilibrium time for BOD<sub>5</sub> and COD removal from greywater with PKAC is 150mins, and removal of BOD<sub>5</sub> and COD from greywater with TAAC is 150mins as shown in Figure 7. This clearly shows that to achieve a greater removal efficiency, PKAC is suitable because it achieves a higher removal percentage at the same equilibrium time. It can be seen from Table 5 that the values of the correlation coefficient ( $R^2$ ) for the pseudo first order model are slightly lower than for the pseudo second order model. The pseudo second order model predicts the sorption behaviour over the whole period of the sorption process. Based on the correlation coefficient values obtained from the pseudo-first-order and pseudo-second-order models, it can be said that the removal of BOD<sub>5</sub> and COD reaction follows a pseudo-second-order kinetics. A pseudo-second order model for BOD<sub>5</sub> and COD removal from waste water was also obtained in a similar study which used activated carbon prepared from date palm (16). Results of kinetic models of similar studies have been presented in Table 6.

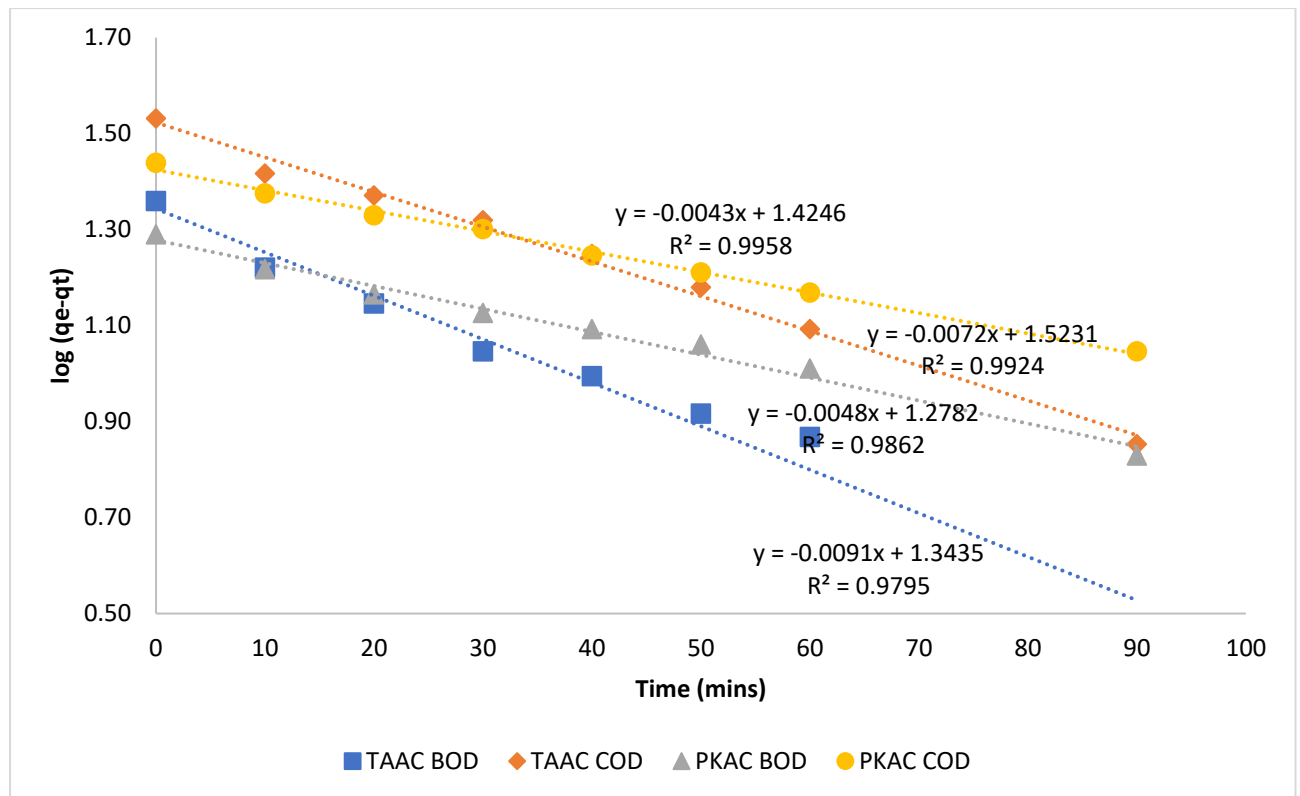


Figure 3. Pseudo-first-order models

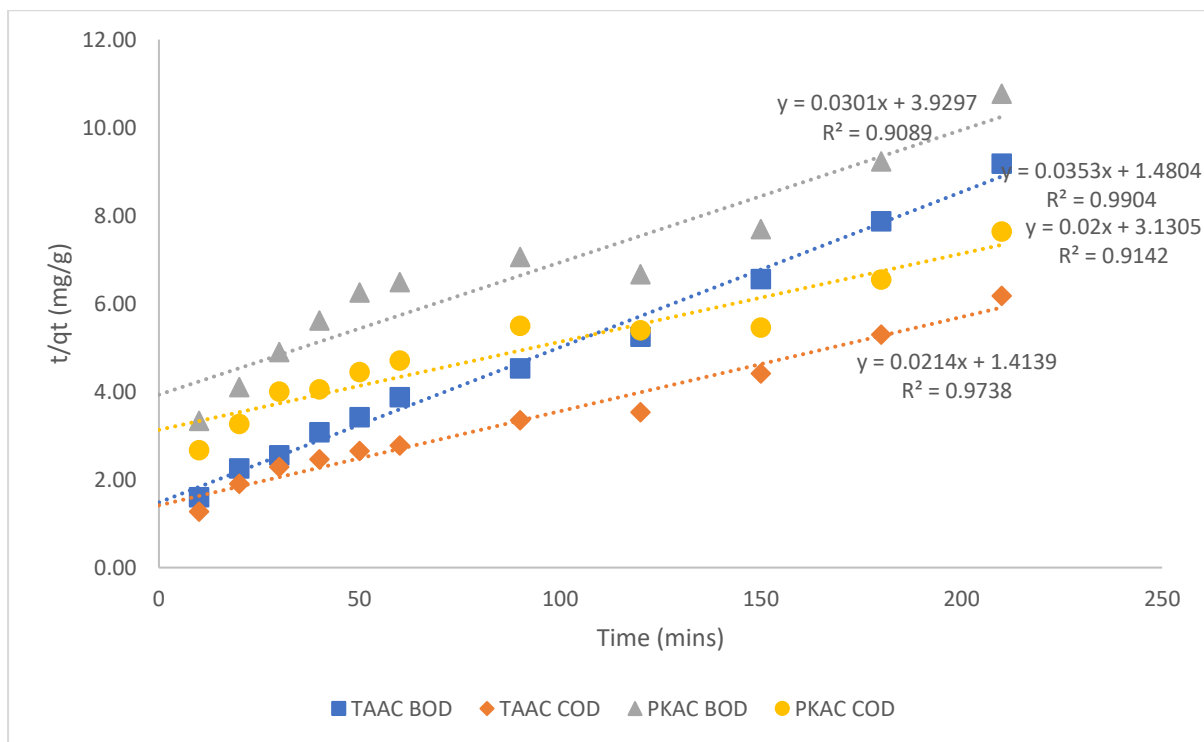


Figure 4. Pseudo-Second-Order models

Table 4. Parameters of pseudo first and second order models

		Pseudo-first-order parameters			Pseudo-second-order parameters			
		$k_1$ ( $\text{min}^{-1}$ ) $\times 10^{-3}$	$q_e$ calc ( $\text{mg g}^{-1}$ )	$R^2$	$k_2$ ( $\text{g mg}^{-1} \text{min}^{-1}$ ) $\times 10^{-5}$	$q_e$ , calc ( $\text{mg g}^{-1}$ )	$h$ ( $\text{mg g}^{-1} \text{min}^{-1}$ )	$R^2$
PKAC	BOD	20.96	22.05	0.9795	84.20	28.33	0.67	0.9904
	COD	16.58	33.35	0.9924	32.40	46.73	0.70	0.9738
TAAC	BOD	11.05	18.97	0.9862	21.10	33.22	0.25	0.9089
	COD	9.90	26.58	0.9958	12.80	50.01	0.32	0.9142

Table 5. Similar Studies

Material (Carbon)	Initial Concentration		Final Concentration		Kinetic model	Adsorption model	Source
	BOD $\text{mg L}^{-1}$	COD $\text{mg L}^{-1}$	BOD $\text{mg L}^{-1}$	COD $\text{mg L}^{-1}$			
Avocado peels	12,000	24,000	98.9	296	-	Freundlich	(28)
Date palm waste	14	38	1	1.75	Pseudo second order	Langmuir and Freundlich	(16)
Animal horns	-	692.57	-	29.99	Pseudo second order	Langmuir and Freundlich	(30)
Fluted pumpkin	3,471	3,959	590.07	514.67	-	-	(35)
Natural Materials	323.3	3,230	14.5	242.3	-	Langmuir and Freundlich	(36)
Tropical Almond	252	421	96	201	Pseudo second order	Freundlich	This study
Palm kernel shell	252	421	69	149	Pseudo second order	Freundlich	This study

## 5. Conclusions

This study explored the adsorption capacity of PKAC and TAAC activated by steam to remove BOD<sub>5</sub> and COD from greywater. The physical characteristics of the materials revealed that activated carbon prepared from PKAC had larger surface area as compared with TAAC. The densities of the materials further revealed that TAAC was very light and may float if used in adsorption process without any aid. However, the density of PKAC was within the recommended densities for activated carbons. The XRD results showed that both materials had no specific functional groups and they were mostly dominated by carbon. The SEM images identified large fan-like structure of the particles of the TAAC while PKAC showed closely packed small particles confirming the high adsorptive capacity of PKAC over TAAC. The experimental results obtained showed that PKAC performed slightly better as compared with TAAC. The PKAC is able to remove 73% BOD<sub>5</sub> and 65% COD while TAAC removed 62% of BOD<sub>5</sub> and 52% COD under the same conditions. The optimum dose of carbon that was obtained

from the study was 8g L<sup>-1</sup> of adsorbent dose and an optimum time of 150mins. The optimum particle was identified to be 2mm for both materials. However, PKAC performs better over TAAC within the same particle size range. It was also established that the adsorption data fitted the Freundlich model well than the other models considered in this study. The adsorption kinetics followed the pseudo-second-order model well more than the pseudo-first-order model. This study indicates that PKAC and TAAC can be used as an adsorbent to remove BOD<sub>5</sub> and COD. The PKAC, however, performs better under the study conditions. The COD concentration in the greywater after treatment makes it suitable for safe disposal into the environment.

## Data Availability Statement

The datasets generated during the current study are available from the corresponding author on reasonable request.

## Conflict of interest

The authors declare no conflict of interest.

## Funding Statement

This work was supported by the Netherlands Government under the NUFFIC project NICHE 194-01 [grant number CF9419].

## Acknowledgments

The authors will like to thank The Netherlands Government for the support.

## References

- [1] Adendorff J, Stimie C. Food from used water - making the previously impossible happen.: South African Research Commission (WRC); 2005 [cited 2017 2nd April]. 23-9]. Available from: [http://journals.co.za/docserver/fulltext/waterb/4/1/waterb\\_v4\\_n1\\_a4.pdf?expires=1493811214&id=id&acname=guest&checksum=510AA057CDF6FD48ADB3BCB40047FFDC](http://journals.co.za/docserver/fulltext/waterb/4/1/waterb_v4_n1_a4.pdf?expires=1493811214&id=id&acname=guest&checksum=510AA057CDF6FD48ADB3BCB40047FFDC).
- [2] Alderlieste, M.; Langeveld, J. Wastewater planning in Djenné, Mali. A pilot project for the local infiltration of domestic wastewater. *Water Sci. Technol.* **2005**, *51*, 57–64, <https://doi.org/10.2166/wst.2005.0032>.
- [3] Boyjoo, Y.; Pareek, V.K.; Ang, M. A review of greywater characteristics and treatment processes. *Water Sci. Technol.* **2013**, *67*, 1403–1424, <https://doi.org/10.2166/wst.2013.675>.
- [4] Busser S, Pham TN, Morel A, Nguyen VA. Characterisitcs and quantities of domestic wastewater in urban and peri-urban households in Hanoi 2006 [Available from: [http://ir.library.osaka-u.ac.jp/dspace/bitstream/11094/13204/1/arfyjsps2006\\_395.pdf](http://ir.library.osaka-u.ac.jp/dspace/bitstream/11094/13204/1/arfyjsps2006_395.pdf)].
- [5] Faraqui N, Al-Jayyousi O. Greywater reuse in urban agriculture for poverty alleviation. A case study in Jordan. *Water International.* 2002;27(3):387-94.
- [6] Oteng-Peprah, M.; de Vries, N.; Acheampong, M. Greywater characterization and generation rates in a peri urban municipality of a developing country. *J. Environ. Manag.* **2018**, *206*, 498–506, <https://doi.org/10.1016/j.jenvman.2017.10.068>.
- [7] Katukiza, A.Y.; Ronteltap, M.; Niwagaba, C.B.; Kansime, F.; Lens, P.N.L. Grey water characterisation and pollutant loads in an urban slum. *Int. J. Environ. Sci. Technol.* **2014**, *12*, 423–436, <https://doi.org/10.1007/s13762-013-0451-5>.
- [8] Oteng-Peprah M, Acheampong MA, deVries NK. Greywater Characteristics, Treatment Systems, Reuse Strategies and User Perception—a Review. *Water, Air, & Soil Pollution.* 2018;229(8):255.
- [9] Edwin, G.A.; Gopalsamy, P.; Muthu, N. Characterization of domestic gray water from point source to determine the potential for urban residential reuse: a short review. *Appl. Water Sci.* **2013**, *4*, 39–49, <https://doi.org/10.1007/s13201-013-0128-8>.

- [10] Eriksson, E.; Auffarth, K.; Eilersen, A.-M.; Henze, M.; Ledin, A. Household chemicals and personal care products as sources for xenobiotic organic compounds in grey wastewater. *Water SA* **2003**, *29*, 135-146, <https://doi.org/10.4314/wsa.v29i2.4848>.
- [11] Ali, I.; Asim, M.; Khan, T.A. Low cost adsorbents for the removal of organic pollutants from wastewater. *J. Environ. Manag.* **2012**, *113*, 170–183, <https://doi.org/10.1016/j.jenvman.2012.08.028>.
- [12] Bansode RR, Losso JN, Marshall WE, Rao RM, Portier RJ. Pecan shell-based granular activated carbon for treatment of chemical oxygen demand (COD) in municipal wastewater. *Bioresource Technol.* 2004;94(2):129-35.
- [13] Hararah, M.A.; Ibrahim, K.A.; Al-Muhtaseb, A.H.; Yousef, R.I.; Abu-Surrah, A.; Qatatsheh, A. Removal of phenol from aqueous solutions by adsorption onto polymeric adsorbents. *J. Appl. Polym. Sci.* **2010**, *117*, 1908–1913, <https://doi.org/10.1002/app.32107>.
- [14] Zhang, Z.; Luo, X.; Liu, Y.; Zhou, P.; Ma, G.; Lei, Z.; Lei, L. A low cost and highly efficient adsorbent (activated carbon) prepared from waste potato residue. *J. Taiwan Inst. Chem. Eng.* **2015**, *49*, 206–211, <https://doi.org/10.1016/j.jtice.2014.11.024>.
- [15] Mohammad-Khah A, Ansari R. Activated charcoal: preparation, characterization and applications: a review article. *Int J Chem Tech.* 2009;1(4):859-64.
- [16] Nayl, A.E.A.; Elkhashab, R.A.; El Malah, T.; Yakout, S.M.; El-Khateeb, M.A.; Ali, M.M.S.; Ali, H.M. Adsorption studies on the removal of COD and BOD from treated sewage using activated carbon prepared from date palm waste. *Environ. Sci. Pollut. Res.* **2017**, *24*, 22284–22293, <https://doi.org/10.1007/s11356-017-9878-4>.
- [17] Hidayu, A.; Muda, N. Preparation and Characterization of Impregnated Activated Carbon from Palm Kernel Shell and Coconut Shell for CO<sub>2</sub> Capture. *Procedia Eng.* **2016**, *148*, 106–113, <https://doi.org/10.1016/j.proeng.2016.06.463>.
- [18] Abdulrazak, S.; Hussaini, K.; Sani, H.M. Evaluation of removal efficiency of heavy metals by low-cost activated carbon prepared from African palm fruit. *Appl. Water Sci.* **2016**, *7*, 3151–3155, <https://doi.org/10.1007/s13201-016-0460-x>.
- [19] Birgani, P.M.; Ranjbar, N.; Abdullah, R.C.; Wong, K.T.; Lee, G.; Ibrahim, S.; Park, C.; Yoon, Y.; Jang, M. An efficient and economical treatment for batik textile wastewater containing high levels of silicate and organic pollutants using a sequential process of acidification, magnesium oxide, and palm shell-based activated carbon application. *J. Environ. Manag.* **2016**, *184*, 229–239, <https://doi.org/10.1016/j.jenvman.2016.09.066>.
- [20] Tze, M.W.; Aroua, M.K.; Szlachta, M. Palm Shell-based Activated Carbon for Removing Reactive Black 5 Dye: Equilibrium and Kinetics Studies. *BioResources* **2015**, *11*, 1432-1447, <https://doi.org/10.15376/biores.11.1.1432-1447>.
- [21] Pamidimukkala, P.S.; Soni, H. Efficient removal of organic pollutants with activated carbon derived from palm shell: Spectroscopic characterisation and experimental optimisation. *J. Environ. Chem. Eng.* **2018**, *6*, 3135–3149, <https://doi.org/10.1016/j.jece.2018.04.013>.
- [22] Lee, J.W.; Chun, J.I.; Jung, H.J.; Kwak, D.H.; Ramesh, T.; Shim, W.G.; Moon, H. Comparative Studies on Coagulation and Adsorption as a Pretreatment Method for the Performance Improvement of Submerged MF Membrane for Secondary Domestic Wastewater Treatment. *Sep. Sci. Technol.* **2005**, *40*, 2613–2632, <https://doi.org/10.1080/01496390500283282>.
- [23] Nasruddin, M.; Fahmi, M.R.; Abidin, C.Z.A.; Yen, T.S. Regeneration of Spent Activated Carbon from Wastewater Treatment Plant Application. **2018**, *1116*, 032022, <https://doi.org/10.1088/1742-6596/1116/3/032022>.
- [24] Oladejo, J.; Shi, K.; Chen, Y.; Luo, X.; Gang, Y.; Wu, T. Closing the active carbon cycle: Regeneration of spent activated carbon from a wastewater treatment facility for resource optimization. *Chem. Eng. Process. - Process. Intensif.* **2020**, *150*, 107878, <https://doi.org/10.1016/j.cep.2020.107878>.
- [25] APHA. Standard methods for the examination of water and wastewater. 21st edition. Washington: American Public Health Association, American Water Works Association, Water Environmental Federation; 2005.
- [26] TIGG L. Granular activated carbon (GAC) media selection Oakdale 2019 [cited 2019 3-January]. Available from: <https://tigg.com/resources/activated-carbon-knowledge-base/granular-activated-carbon-gac-media-selection/>.
- [27] ICDD. Powder diffraction file: JCPDS-ICDD; 2018 [cited 2019 10/3].
- [28] Devi, R.; Singh, V.; Kumar, A. COD and BOD reduction from coffee processing wastewater using Avacado peel carbon. *Bioresour. Technol.* **2008**, *99*, 1853–1860, <https://doi.org/10.1016/j.biortech.2007.03.039>.
- [29] Mangaleswaran, L.; Thirulogachandar, A.; Rajasekar, V.; Muthukumaran, C.; Rasappan, K. Batch and fixed bed column studies on nickel (II) adsorption from aqueous solution by treated polyurethane foam. *J. Taiwan Inst. Chem. Eng.* **2015**, *55*, 112–118, <https://doi.org/10.1016/j.jtice.2015.03.034>.
- [30] Aluyor EO, Oboh IO, Obahiagbon KO. Equilibrium sorption isotherm for lead (Pb) ions on hydrogen peroxide modified rice hulls. *Int J Phys Sci.* 2009;4(8):423-7.



- [31] Ghana. E. General Environmental Quality standards. Ghana: EPA; 2000.
- [32] Belhachemi M, Addoun F. Adsorption of congo red onto activated carbons having different surface properties: studies of kinetics and adsorption equilibrium. *Desalin Water Treat.* 2012;37(1-3):122-9.
- [33] Yan, H.; Du, X.; Li, P.; Yu, S.; Tang, Y. Adsorption of bromate from aqueous solutions by modified granular activated carbon: batch and column tests. *Ozone: Sci. Eng.* **2015**, *37*, 357–370, <https://doi.org/10.1080/01919512.2014.1001020>.
- [34] Acheampong, M.A.; Pereira, J.P.; Meulepas, R.J.; Lens, P.N. Biosorption of Cu(II) onto agricultural materials from tropical regions. *J. Chem. Technol. Biotechnol.* **2011**, *86*, 1184–1194, <https://doi.org/10.1002/jctb.2630>.
- [35] Wirnkor VA, Amonia BO, Ngozi VE. Batch and Column Adsorption of BOD and COD in vegetable oil industry effluents Using Activated Carbon from Fluted Pumpkin (*Telfairia, Occidentalis*. Hook. F) Seed Shell. *International Letters of Chemistry, Physics and Astronomy.* 2014;20 (1):64-77.
- [36] Patel H, Vashi RT. COD and BOD Removal from Textile Wastewater using Natural Materials. *International Journal of Applied Environmental Sciences.* 2010;2:179 - 88.